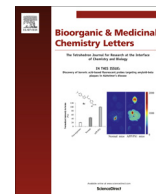




Contents lists available at ScienceDirect

Bioorganic & Medicinal Chemistry Letters

journal homepage: www.elsevier.com/locate/bmcl

Synthesis and antiproliferative activity of 6,7-disubstituted-4-phenoxyquinoline derivatives bearing the 2-oxo-4-chloro-1,2-dihydroquinoline-3-carboxamide moiety

Qidong Tang^{a,b,*,†}, Xin Zhai^{b,†}, Yayi Tu^a, Ping Wang^a, Linxiao Wang^a, Chunjiang Wu^a, Wenhui Wang^a, Hongbo Xie^c, Ping Gong^b, Pengwu Zheng^{a,*}

^a School of Pharmacy, Jiangxi Science and Technology Normal University, Nanchang, Jiangxi 330013, PR China

^b Key Laboratory of Structure-Based Drug Design and Discovery of Ministry of Education, School of Pharmaceutical Engineering, Shenyang Pharmaceutical University, Shenyang 110016, PR China

^c College of Bioinformatics Science and Technology, Harbin Medical University, Harbin 150081, PR China

ARTICLE INFO

Article history:

Received 20 January 2016

Revised 10 February 2016

Accepted 15 February 2016

Available online 15 February 2016

Keywords:

Synthesis

Quinoline derivatives

2-Oxo-4-chloro-1,2-dihydroquinoline

c-Met

Antiproliferative activity

ABSTRACT

A series of 6,7-disubstituted-4-phenoxyquinoline derivatives bearing the 2-oxo-4-chloro-1,2-dihydroquinoline-3-carboxamide moiety were synthesized, and evaluated for their antiproliferative activity against 5 cancer cell lines (H460, HT-29, MKN-45, A549, and U87MG). Most compounds showed moderate to excellent potency, and compared to foretinib, the most promising analog **42** (c-Met/Flt-3 IC₅₀ = 1.21/2.15 nM) showed a 6.1-fold increase in activity against H460 cell line in vitro. The enzymatic assays (c-Met, VEGFR-2, Flt-3, PDGFR-β, c-Kit, and EGFR) of compound **42** were evaluated in vitro. Docking analysis showed that compound **42** could form three hydrogen bonds with c-Met. Structure-activity relationship studies indicated that a more water-soluble cyclic tertiary amine and electron-withdrawing groups at 4-position of the phenyl ring contribute to the antitumor activity.

© 2016 Elsevier Ltd. All rights reserved.

Cancer is a widespread, complex, and lethal disease. There were 14.1 million new cancer cases, 8.2 million deaths and 32.6 million people living with cancer (within 5 years of diagnosis) in 2012 worldwide.¹ Despite the efforts to discover and develop small molecule anticancer drugs in the last decade,^{2–5} development of new antitumor agents with improved tumor selectivity, efficiency, and safety remains desirable.

Recently, a number of new quinoline derivatives with excellent antitumor activity have been reported.^{6–14} Among them, 6,7-disubstituted (or 7-substituted)-4-aryloxyquinoline derivatives, which could inhibit c-Met kinase, have attracted our attention. Many of these derivatives are already being marketed or are under clinical/preclinical studies, such as cabozantinib, foretinib, AMG458, MG10, Amgen, and AM7 (**1–6**, Fig. 1). The main modification of these quinoline derivatives was focused on the 5-atom linker between moiety A and moiety B, which was characterized by the illustrated '5 atoms regulation' or 'hydrogen-bond donor or acceptor' in our previous work.^{15,16}

* Corresponding authors. Tel./fax: +86 791 83802393.

E-mail addresses: tangqidongcn@126.com (Q. Tang), zhengpw@126.com (P. Zheng).

[†] These authors contribute equally to this work.

In our previous study, we introduced 1,4-dihydrocinnoline and quinoline fragment as part of the 5-atom linker, and the resulting derivatives *N*-(3-fluoro-4-(6,7-disubstitutedquinolin-4-yloxy)phenyl)-4-oxo-1-(substitutedphenyl)-1,4-dihydrocinnoline-3-carboxamides (**7**, Fig. 2) and *N*-(3-fluoro-4-(6,7-disubstitutedquinolin-4-yloxy)phenyl)-2-substitutedphenylquinoline-4-carboxamides (**8**, Fig. 2) showed excellent potency.^{15,16} 2-oxo-1,2-dihydroquinoline fragment is widely used as a building block in drug design because of its ability to form hydrogen-bonding interactions with drug targets, such as **H₂L** (**9**, Fig. 2)¹⁷ which could interact with CT-DNA through intercalation.

Taking foretinib as the leading compound, we introduced the 2-oxo-4-chloro-1,2-dihydroquinoline-3-carboxamide moiety to foretinib as the 5-atom linker (Fig. 3) based on the illustrated '5 atoms regulation' and 'hydrogen-bond donor or acceptor' to make further study. The 3-carbon tether at the 7 position of quinoline was reserved, while the morpholinyl group was replaced by four other water-soluble substituents based on our previous study,¹⁸ including pyrrolidinyl, piperidinyl, 4-methyl piperidinyl, and 4-methyl piperazinyl groups, to observe the effects of the different cyclic tertiary amino groups on activity of the new compounds. Furthermore, various substituents were introduced at the phenyl ring (moiety B) to investigate their effects on activity.

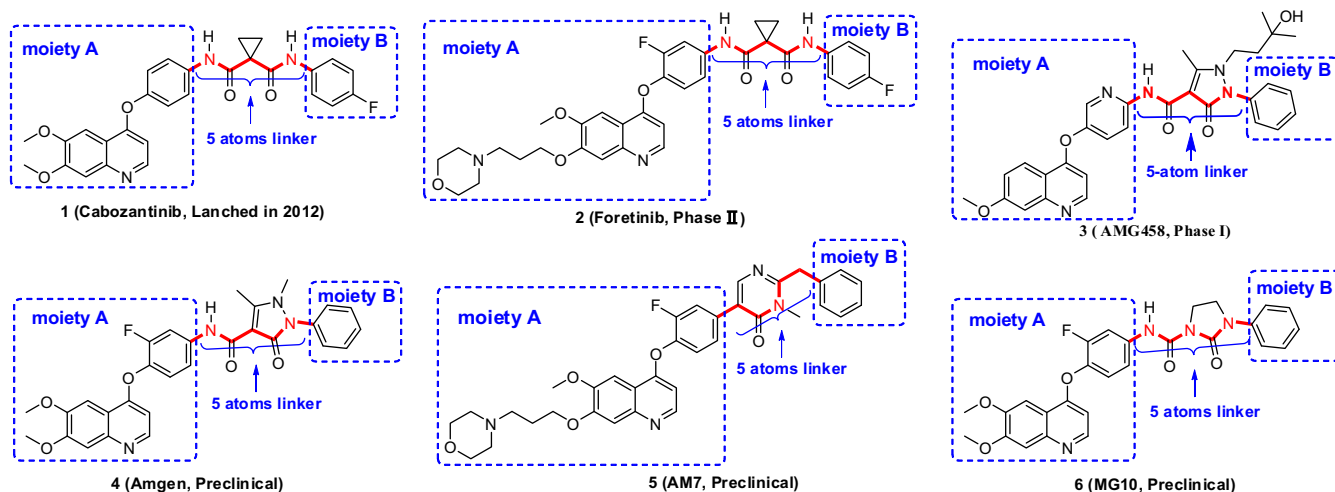


Figure 1. The representative small-molecule c-Met kinase inhibitors.

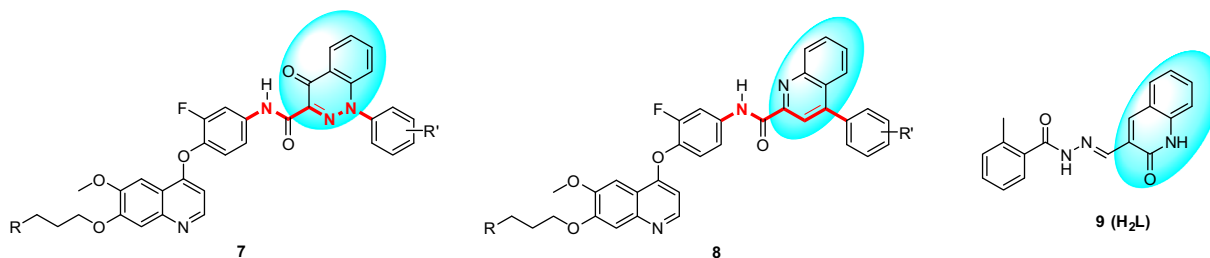


Figure 2. Our previous work on antiproliferative agents bearing quinoline scaffolds and H₂L.

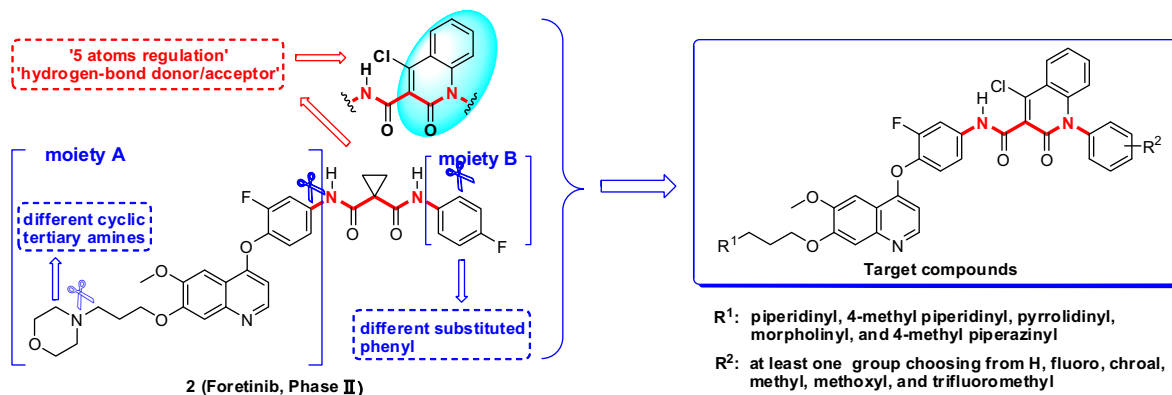


Figure 3. Design strategy for the quinoline derivatives bearing 2-oxo-4-chloro-1,2-dihydroquinoline moiety.

Accordingly, we designed a novel series of 6,7-disubstituted-4-phenoxyquinoline derivatives bearing 2-oxo-4-chloro-1,2-dihydroquinoline-3-carboxamide moiety.

The antiproliferative effect of all the 23 newly synthesized compounds on the growth of five cell lines, namely human lung cancer (H460), human colon cancer (HT-29), human lung adenocarcinoma (A549), human gastric cancer (MKN-45), and human glioblastoma (U87MG) overexpression, was evaluated *in vitro*.^{19–21} Apparent growth inhibition was observed for most of the compounds, and 12 of these compounds were more potent than foretinib against one or more cell lines. Furthermore, eight compounds were chosen for further evaluation of c-Met kinase inhibitory activity *in vitro*. To examine the selectivity of compound **42** on c-Met over other tyrosine

kinases. To further elucidate the binding mode of compounds with c-Met kinase, docking analysis was performed using compound **42**.

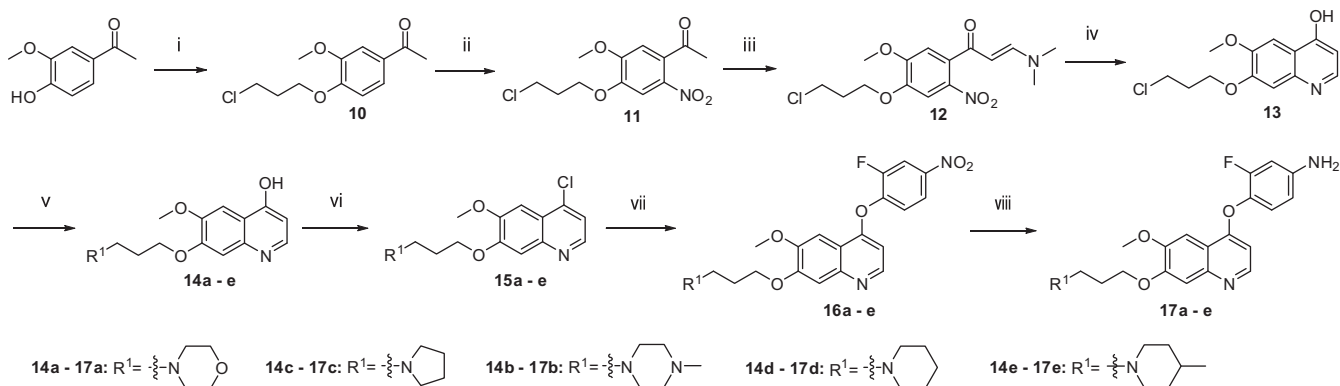
The synthesis of the key intermediates of 6,7-disubstituted-4-phenoxyquinolines **17a–e** was achieved in 8 steps from commercially available 1-(4-hydroxy-3-methoxyphenyl)ethanone as shown in Scheme 1, which has been illustrated in detail in our previous study.¹⁵

The target compounds **23–45** were prepared as illustrated in Scheme 2. Using Cu and Cu₂O as catalyst, Ullmann reaction of commercially 2-chlorobenzoic acid with substituted phenylamines in ethylene glycol at 170 °C yielded intermediates **18a–g**.²² Acylation of **18a–g** with triphosgene in the presence of potassium carbonate (K₂CO₃) in ethyl acetate resulted in high yield of intermediates **19a–g**, which were condensed with dimethyl malonate in the

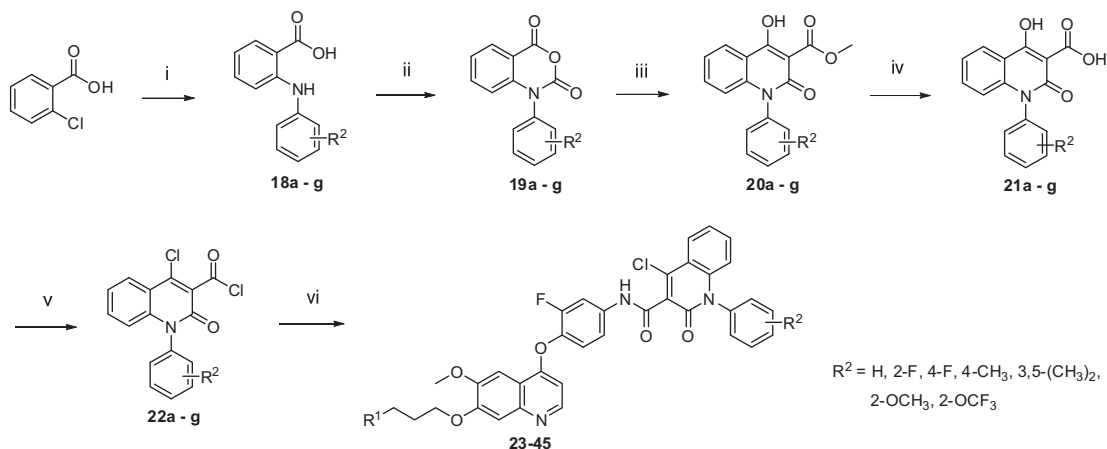
presence of sodium methylate (NaOCH₃) in hot dimethyl formamide (DMF) to afford intermediates **20a–g**.²³ Simple procedures such as hydrolysis and acyl chlorination were used to convert **20a–g** to the corresponding acyl chlorides **22a–g**; the reactions proceeded with AcOH/HCl (concd) and thionyl chloride,

respectively. Reaction of amides **17a–e** with acyl chlorides **22a–g** promoted by DIPEA in dichloromethane at room temperature yielded the target compounds **23–45**.¹⁵

The cytotoxic activity of targeted compounds was listed in Table 1.²⁴ All the 23 newly synthesized target compounds (**23–45**)



Scheme 1. Reagents and conditions: (i) Br(CH₂)₃Cl, acetone, 0 °C, 30 min, rt, 12 h; (ii) 98% HNO₃, CH₂Cl₂, 0 °C, 4 h; (iii) DMF–DMA, toluene, 110 °C, 10 h; (iv) Fe powder, AcOH, rt, 30 min, 80 °C, 2 h; (v) secondary amines, CH₃CN, 85 °C, 10 h; (vi) POCl₃, 85 °C, 6 h; (vii) 2-fluoro-4-nitrophenol, PhCl, 140 °C, 30 h; (viii) Fe powder, NH₄Cl (cat.), EtOH/H₂O, reflux, 5 h.



Scheme 2. Reagents and conditions: (i) appropriate aniline, Cu, Cu₂O, K₂CO₃, ethylene glycol, 170 °C, 24–30 h; (ii) triphosgene, K₂CO₃, ethyl acetate, rt, 6–10 h; (iii) dimethyl malonate, CH₃ONa, DMF, N₂, 50 °C, 0.5 h, 85 °C, 30 min; (iv) AcOH, HCl (concd), 80 °C, 3 h; (v) SOCl₂, reflux, 6 h; (vi) appropriate aniline, DIPEA, CH₂Cl₂, 0 °C, 1 h, rt, 15–20 h.

Table 1

Cytotoxic activities of the target compounds **23–45** against the H460, HT-29, MKN-45, A549, and U87MG cancer cell lines in vitro

Compd	R ¹	R ²	IC ₅₀ (μM)				
			H460	HT-29	MKN-45	A549	U87MG
23		H	0.26 ± 0.063	0.46 ± 0.025	0.31 ± 0.052	0.93 ± 0.064	4.8 ± 0.26
24		4-F	0.061 ± 0.0050^a	0.14 ± 0.016	0.21 ± 0.040	0.11 ± 0.030	8.5 ± 0.50
25		2-F	0.58 ± 0.032	1.21 ± 0.33	0.74 ± 0.063	ND ^b	ND
26		4-CH ₃	0.85 ± 0.026	0.39 ± 0.014	0.78 ± 0.080	0.83 ± 0.041	5.16 ± 0.23
27		2-OCH ₃	1.2 ± 0.26	1.4 ± 0.19	1.26 ± 0.081	ND	ND
28		H	0.21 ± 0.022	0.39 ± 0.028	0.21 ± 0.030	0.81 ± 0.032	1.6 ± 0.18
29		4-F	0.12 ± 0.080	0.15 ± 0.021	0.57 ± 0.042	0.72 ± 0.060	0.64 ± 0.045
30		4-CH ₃	0.23 ± 0.031	0.48 ± 0.036	0.90 ± 0.014	0.23 ± 0.057	3.24 ± 0.16
31		3,5-(CH ₃) ₂	0.62 ± 0.015	0.30 ± 0.029	1.2 ± 0.26	ND	ND
32		2-OCF ₃	0.36 ± 0.031	1.5 ± 0.16	1.4 ± 0.20	ND	ND
33		H	0.14 ± 0.07	41.6 ± 0.23	0.28 ± 0.063	0.51 ± 0.040	1.3 ± 0.10
34		4-F	0.11 ± 0.058	0.29 ± 0.051	0.31 ± 0.032	0.16 ± 0.025	1.6 ± 0.18
35		4-CH ₃	0.17 ± 0.030	0.52 ± 0.062	0.48 ± 0.020	ND	ND
36		2-OCH ₃	0.58 ± 0.04	12.6 ± 0.31	0.42 ± 0.025	ND	ND

Table 1 (continued)

Compd	R ¹	R ²	IC ₅₀ (μM)				
			H460	HT-29	MKN-45	A549	U87MG
37		H	0.15 ± 0.075	0.35 ± 0.048	0.46 ± 0.053	0.39 ± 0.022	1.42 ± 0.43
38		4-F	0.089 ± 0.0046	0.11 ± 0.037	0.16 ± 0.046	0.99 ± 0.024	1.92 ± 0.72
39		4-CH ₃	0.18 ± 0.0070	0.19 ± 0.039	0.12 ± 0.082	0.35 ± 0.036	3.2 ± 0.37
40		2-OCF ₃	0.38 ± 0.030	0.57 ± 0.062	0.31 ± 0.032	ND	ND
41		H	0.061 ± 0.052	0.091 ± 0.0035	0.12 ± 0.087	ND	ND
42		4-F	0.031 ± 0.0053	0.068 ± 0.0082	0.16 ± 0.037	0.11 ± 0.024	0.52 ± 0.31
43		2-F	0.27 ± 0.058	0.17 ± 0.034	0.41 ± 0.021	0.29 ± 0.036	1.32 ± 0.25
44		4-CH ₃	0.12 ± 0.041	0.15 ± 0.025	0.12 ± 0.015	0.31 ± 0.060	1.06 ± 0.27
45		2-OCH ₃	0.15 ± 0.041	0.53 ± 0.084	0.12 ± 0.015	ND	ND
Foretinib ^c			0.19 ± 0.036	0.16 ± 0.015	0.032 ± 0.0052	0.13 ± 0.010	1.1 ± 0.12

^a Bold values show the IC₅₀ values of the target compounds lower than the values of the positive control.

^b ND: not determined.

^c Used as the positive control.

Table 2

c-Met kinase activity of selected compounds **24**, **29**, **33**, **34**, **37**, **38**, **41**, **42** and foretinib in vitro

Compd	IC ₅₀ on c-Met (nM)
24	5.32
29	12.51
33	18.39
34	12.18
37	6.84
38	3.26
41	1.75
42	1.21
Foretinib	1.84

Table 3

Inhibition of tyrosine kinases by compound **42**

Kinase	Enzyme IC ₅₀ (nM)
Flt-3	2.15
c-Kit	362.8
PDGFR-β	526.5
VEGFR-2	542.6
EGFR	>100,000

showed moderate to excellent cytotoxic activity against the five tested cancer cells with potencies in the single digit μM range, which suggested that replacement of *N*-(4-fluorophenyl)cyclo-

propane-1,1-dicarboxamide framework of foretinib with 2-oxo-4-chloro-1,2-dihydroquinoline-3-carboxamide moiety maintained the potent cytotoxic activity. The IC₅₀ values of the most promising compound **42**²⁵ were 0.031 μM, 0.068 μM, and 0.52 μM against H460, HT-29, and U87MG cell lines, respectively; these values indicated that this compound was 6.1, 2.4, and 2.1 times more active than foretinib (IC₅₀ values: 0.19 μM, 0.16 μM, and 1.1 μM, respectively). In addition, most of the compounds displayed higher selectivity against H460 and HT-29 cells than against the other three cell lines.

The cell lines data revealed a clear preference for activity when the R¹ group was 4-methyl piperazinyl group, which indicated that a more water-soluble cyclic tertiary amino group at the 7 position of quinoline contributed to the potency of the target compounds. For example, the IC₅₀ value of compound **41** (R¹ = 4-methyl piperazinyl), 0.061 μM, was clearly lower than that of **23**, **28**, **33**, and **37**, 0.26 μM, 0.21 μM, 0.14 μM, and 0.15 μM, respectively, against H460 cells.

Further analysis clearly revealed that different cytotoxic activities were observed when various R² groups were introduced into the phenyl ring (moiety B). Compound **23**, with no substituent on the phenyl ring, displayed strong cytotoxicity with an IC₅₀ of 0.26 μM against H460 cells. The introduction of electron-withdrawing groups at 4-position of the phenyl ring (**24**, R² = 4-F, IC₅₀ = 0.061 μM) led to an obvious improvement in antitumour activity, which could be further confirmed by compounds **29**, **34**,

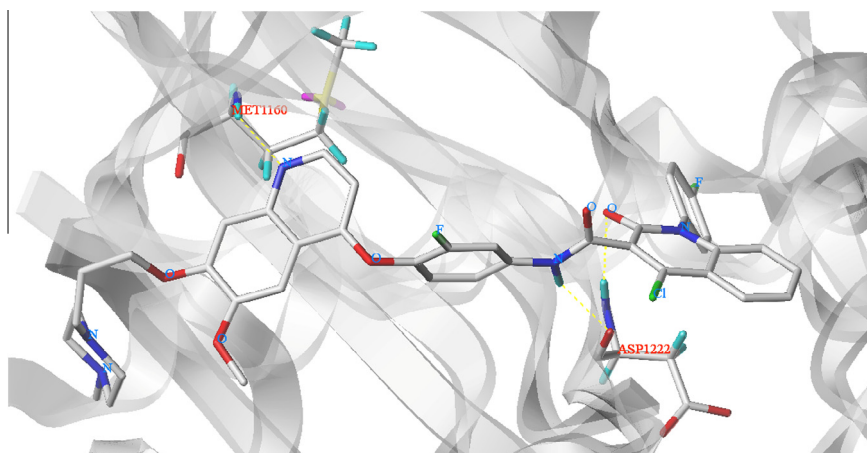


Figure 4. Binding poses of compound **42** with c-Met. The proteins were displayed by grid ribbon. Compound **42** were displayed by multicolor sticks. H-bonding interactions between the **42** and c-Met were indicated with dashed lines in yellow.

38, and **42**. However, the introduction of electron-withdrawing (**25**, 2-F, IC_{50} = 0.82 μ M) or electron-donating groups (**27**, 2-OCH₃, IC_{50} = 1.2 μ M) at other position reduced the activities.

The c-Met enzymatic assays of eight compounds were evaluated using homogeneous time-resolved fluorescence (HTRF) assay and showed excellent result,²⁶ which suggested that the inhibition of c-Met may be one mechanism of the antiproliferative effect of these derivatives (Table 2). Compound **42** showed the most potent activity with an IC_{50} value of 1.21 nM, which was superior to that of the positive control foretinib (IC_{50} = 1.84 nM), and this compound should be studied further.

Compound **42** were chosen for further evaluation the selectivity on c-Met over other tyrosine kinases.¹⁶ As shown in Table 3, compared with its high potency against c-Met (IC_{50} = 1.21 nM), **42** also exhibited high inhibitory effects against Flt-3 (IC_{50} = 2.15 nM). While, **42** showed weak potency on c-Kit, VEGFR-2, PDGFR- β , and EGFR. These data suggested that compound **42** had a selectivity on c-Met and Flt-3.

To further elucidate the binding mode of compounds, docking analysis was performed. In our study, the co-crystal structure of foretinib with c-Met kinase was selected as the docking model (PDB ID: 3LQ8). The docking simulation was conducted using SURFLEX-DOCK module of SYBYL 6.9.1 package version. As depicted in Figure 4, the shape and properties of the receptor are represented on a grid by several different sets of fields that provide progressively more accurate scoring of the ligand poses. The binding model was exemplified by the interaction of compound **42** with c-Met. As shown in Figure 4, the nitrogen atom of the quinoline ring in **42** formed hydrogen-bonding interactions with MET1160. The hydrogen atom of the amido linkage and the oxygen atom of the 2-oxo-4-chloro-1,2-dihydroquinoline formed two hydrogen bonds with ASP1222. The result demonstrated that compound **42** could form three hydrogen bonds with c-Met.

In summary, we designed and synthesized 23 quinoline derivatives bearing a 2-oxo-4-chloro-1,2-dihydroquinoline-3-carboxamide moiety. Five human cell lines were used to evaluate the potency of the synthesized compounds, and 12 of these derivatives were more potent than foretinib. Compound **42** (c-Met/Flt-3 IC_{50} = 1.21/2.15 nM) showed the strongest cytotoxic activities against H460, HT-29, and U87MG cell lines which was 6.1, 2.4, and 2.1 times more active than foretinib against the 3 cell lines, respectively. Docking analysis showed that compound **42** could form three hydrogen bonds with c-Met. The analysis of SARs indicated that a more water soluble cyclic tertiary amine (R^1 = 4-methyl piperazinyl) contributed to the potency. Electron-withdrawing groups at 4-position (R^2 = 4-F) of the phenyl ring contribute to the antiproliferative activity. Further studies on SARs and mechanism of action of these compounds are in progress, and their results will be reported in the future.

Acknowledgment

This work was supported by National Natural Science Foundation of China (NSFC No. 81573295).

Supplementary data

Supplementary data associated with this article can be found, in the online version, at <http://dx.doi.org/10.1016/j.bmcl.2016.02.037>.

References and notes

- <http://www.who.int/mediacentre/factsheets/fs297/en/> (WHO Media Centre, Cancer, updated Feb, 2015, last accessed: 10/30/2015).
- Samadi, A. K.; Bazzill, J.; Zhang, X.; Gallagher, R.; Zhang, H. P.; Gollapudi, R.; Kindscher, K.; Timmermann, B.; Cohen, M. S. *Surgery* **2012**, *152*, 1238.
- You, W. K.; Sennino, B.; Williamson, C. W.; Falcón, B.; Hashizume, H.; Yao, L. C.; Aftab, D. T.; McDonald, D. M. *Cancer Res.* **2011**, *71*, 4758.
- Dayyani, F.; Gallick, G. E.; Christopher, C. L.; Corn, P. G. *J. Natl Cancer Inst.* **2011**, *103*, 1665.
- Hoelder, S.; Clarke, P. A.; Workman, P. *Mol. Oncol.* **2012**, *6*, 155.
- Kung, P. P.; Funk, L.; Meng, J.; Altton, G.; Padrique, E.; Mroczkowski, B. *Eur. J. Med. Chem.* **2008**, *43*, 1321.
- Yakes, F. M.; Chen, J.; Tan, J.; Yamaguchi, K.; Shi, Y. C.; Yu, P. W.; Qian, F.; Chu, F.; Bentzien, F.; Cancilla, B.; Orf, J.; You, A.; Laird, A. D.; Engst, S.; Lee, L.; Lesch, J.; Chou, Y. C.; Joly, A. H. *Mol. Cancer Ther.* **2011**, *10*, 2298.
- Norman, M. H.; Liu, L. B.; Lee, M.; Xi, N.; Fellows, I.; D'Angelo, N. D.; Dominguez, C.; Rex, K.; Bellon, S. F.; Kim, T. S.; Dussault, I. *J. Med. Chem.* **2012**, *55*, 1858.
- Cecchi, F.; Rabe, D. C.; Bottaro, D. P. *Eur. J. Cancer* **2010**, *46*, 1260.
- Liu, X. D.; Newton, R. C.; Scherle, P. A. *Trends Mol. Med.* **2009**, *16*, 1471.
- Kataoka, Y.; Mukohara, T.; Tomioka, H.; Funakoshi, Y.; Kiyota, N.; Fujiwara, Y.; Yashiro, M.; Hirakawa, K.; Hirai, M.; Minami, H. *Invest. New Drugs* **2012**, *30*, 1352.
- González-Sánchez, I.; Solano, J. D.; Loza-Mejía, M. A.; Olvera-Vázquez, S.; Rodríguez-Sotres, R.; Morán, J.; Lira-Rocha, A.; Cerbón, M. A. *Eur. J. Med. Chem.* **2011**, *46*, 2102.
- Li, S.; Liang, Y. J.; Liu, J. C.; He, H. W.; Chen, Y.; Tang, C.; Yang, G. Z.; Fu, L. W. *Eur. J. Med. Chem.* **2012**, *47*, 206.
- Abonia, R.; Insuasty, D.; Castillo, J.; Insuasty, B.; Quiroga, J.; Nogueras, M.; Cobo, J. *Eur. J. Med. Chem.* **2012**, *57*, 29.
- Li, S.; Huang, Q.; Liu, Y. J.; Zhang, X. L.; Liu, S.; He, C.; Gong, P. *Eur. J. Med. Chem.* **2013**, *64*, 62.
- Li, S.; Zhao, Y. F.; Wang, K. W.; Gao, Y. L.; Han, J. M.; Cui, B. B.; Gong, P. *Bioorg. Med. Chem.* **2013**, *21*, 2843.
- Duraisamy, S. R.; Eswaran, R.; Nattamai, S. P.; Karuppannan, N. *Eur. J. Med. Chem.* **2013**, *64*, 148.
- Tang, Q. D.; Zhao, Y. F.; Du, X. M.; Chong, L. E.; Gong, P.; Guo, C. *Eur. J. Med. Chem.* **2013**, *69*, 77.
- Tiedt, R.; Degenkolbe, E.; Furet, P.; Appleton, B. A.; Wagner, S.; Schoepfer, J.; Buck, E.; Ruddy, D. A.; Monahan, J. E.; Jones, M. D.; Blank, J.; Haasen, D.; Druce, P.; Wartmann, M.; McCarthy, C.; Sellers, W. R.; Hofmann, F. *Cancer Res.* **2011**, *71*, 5255.
- Ted, L. U.; Torsten, H.; Sheila, J. M. *Anticancer Agents Med.* **2010**, *10*, 7.
- Takayuki, N.; Osamu, T.; Atsumi, Y.; Tomohiro, M.; Keiko, T.; Setsuo, F.; Shuji, S.; Makoto, A.; Hiroshi, O. *Cancer Sci.* **2010**, *101*, 210.
- Martin, A.; Mesa, M.; Docampo, M. L. *Synth. Commun.* **2006**, *36*, 271.
- Jönsson, S.; Andersson, G.; Fex, T. *J. Med. Chem.* **2004**, *47*, 2075.
- Cytotoxicity assay:** A standard MTT assay was used to measure cell growth. The cancer cell lines were cultured in minimum essential medium (MEM) supplemented with 10% fetal bovine serum (FBS). Approximately 4×10^3 cells, suspended in MEM medium, were plated onto each well of a 96-well plate and incubated in 5% CO₂ at 37 °C for 24 h. The compounds tested at the indicated final concentrations were added to the culture medium and the cell cultures were continued for 72 h. Fresh MTT was added to each well at a terminal concentration of 5 μ g/mL, and incubated with cells at 37 °C for 4 h. The formazan crystals were dissolved in 100 μ L DMSO of each well, and the absorbency at 492 nm (for absorbance of MTT formazan) and 630 nm (for the reference wavelength) was measured with an ELISA reader. All of the compounds were tested in triplicate in each cell line. The results expressed as IC_{50} (inhibitory concentration 50%) were the averages of three determinations and calculated by using the Bacus Laboratories Incorporated Slide Scanner (Bliss) software.
- Analytic data of potent inhibitor 42:** ¹H NMR (300 MHz, CDCl₃) δ 11.12 (s), 8.63 (d, J = 5.2, 1H), 8.06 (dd, J = 12.1, 2.4 Hz, 1H), 7.87 (d, J = 8.4, 1H), 7.81–7.75 (m, 2H), 7.59 (s), 7.48 (d, J = 8.4, 1H), 7.43 (s), 7.41–7.25 (m, 6H), 6.41 (d, J = 5.4, 1H), 4.26 (t, J = 6.8 Hz, 2H), 4.03 (s, 3H), 2.66–2.52 (m, 4H), 2.47 (br, 6H), 2.27 (s, 3H), 2.15–2.03 (m, 2H); ¹³C NMR (150 MHz, CDCl₃) 164.89, 161.32, 159.52, 158.17, 155.36, 153.26, 152.11, 150.12, 149.16, 147.83, 146.12, 142.48, 139.35, 136.91, 136.29, 134.82, 133.84, 131.14, 129.28 (2C), 128.64, 125.95, 124.26, 123.91, 116.45, 116.21, 110.35, 109.73, 108.62, 102.84, 99.65, 67.54, 56.22, 55.25 (2C), 54.82, 53.09 (2C), 46.36, 26.42; MS m/z (ESI): 740.4 [M+H]⁺; Anal. calcd for C₄₀H₃₆F₂ClN₅O₅: C, 64.91; H, 4.90; N, 9.46. Found: C, 64.89; H, 4.88; N, 9.41.
- In vitro kinase assay:** The kinase assays were performed by homogeneous time-resolved fluorescence (HTRF) assay as previously reported protocol. Briefly, 20 μ g/mL poly (Glu, Tyr) 4:1 (Sigma) was preloaded as a substrate in 384-well plates. Then 50 μ L of 10 mM ATP (Invitrogen) solution diluted in kinase reaction buffer (50 mM HEPES, pH 7.0, 1 M DTT, 1 M MgCl₂, 1 M MnCl₂, and 0.1% NaN₃) was added to each well. Various concentrations of compounds diluted in 10 μ L of 1% DMSO (v/v) were used as the negative control. The kinase reaction was initiated by the addition of purified tyrosine kinase proteins diluted in 39 μ L of kinase reaction buffer solution. The incubation time for the reactions was 30 min at 25 °C, and the reactions were stopped by the addition of 5 μ L of Streptavidin-XL665 and 5 μ L Tk Antibody Cryptate working solution to all of wells. The plates were read using Envision (PerkinElmer) at 320 nm and 615 nm. The inhibition rate (%) was calculated using the following equation: % inhibition = 100 – [(Activity of enzyme with tested compounds – Min)/(Max – Min)] \times 100 (Max: the observed enzyme activity measured in the presence of enzyme, substrates, and cofactors; Min: the observed enzyme activity in the presence of substrates, cofactors and in the absence of enzyme). IC_{50} values were calculated from the inhibition curves.